Effect of Ti Addition to Age Hardening Response of Al-10Zn-6Mg-xTi Alloy Produced by Squeeze Casting

Dwi Ayu Nurcahyaningsih[1], *Risly* Wijanarko[1], *Irene* Angela[1], and *Bondan* Tiara Sofyan[1]

[1]Department of Metallurgy and Materials Engineering, Faculty of Engineering, Universitas of Indonesia, Depok 16424, West Java, Indonesia

Abstract. This research focused on investigating the effects of Ti addition on the age hardening response of Al 7xxx alloy for Organic Rankine Cycle (ORC) turbine impeller application in power plant generators. Al-10Zn-6Mg wt. % alloys were produced by squeeze casting with 0.02, 0.05, and 0.25 wt. % Ti addition. As-cast samples were homogenized at 400 ^{o}C for 4 h. Solution treatment was conducted at 440 ^{o}C for 1 h, followed by quenching and ageing at 130 ^{o}C for 200 h. Age hardening result was observed using Rockwell B hardness measurement. Other characterizations included impact testing, STA, optical microscopy, and SEM-EDS. Results showed that the addition **of** Ti in all content variations increased the as-cast hardness due to the diminution of secondary dendrite arm spacing (SDAS) values of the alloy. Ageing at 130 ^{o}C strengthened the alloys, however the addition of Ti was not found to affect neither peak hardness nor impact values of the alloy. Identities of second phases formed during solidification were found to be T ($Mg_{32}(Al,Zn)_{49}$), β (Al_8Mg_5), and $TiAl_3$, while precipitates produced during ageing were GP Zone, η', and η ($MgZn_2$). **Keywords –** ageing, Al-Zn-Mg, grain refining, $MgZn_2$, Ti addition.

1 Introduction

Al 7xxx alloys with its Zn and Mg alloying content are commonly used for high temperature service. The alloy is currently developed for turbine impeller application in novel Organic Rankine Cycle/ORC power generating system considering its lightweight, strong, and durable properties [1] that would contribute positively to the overall system efficiency.

Grain refining agents – e.g. Ti, Cr, Zr, or other rare earth elements are used in order to further strengthen the alloy. Kurniawan [2] founded that 0.067, 0.081, and 0.115 wt. % Ti content in AC4B alloy all resulted in increased strength and UTS value of the alloy. Addition of 0.050 and 0.072 wt. % Ti was also evident to be able to optimize the hardness of AC4B alloy by 2.80 % and 7.17 %, along with optimizing its tensile strength by 4.40 % and 5.10 % compared to those without Ti addition. The strengthening mechanism was a result of primary α-Al grain refining phenomenon followed by a decrease in dendrite arm spacing/DAS value [3]. Heterogeneous nucleation and grain boundary strengthening effect were also found after 0.058, 0.073, and 0.104 wt. % Ti addition to both squeeze-cast and aged Al-9Zn-6Mg-2Si wt. % alloy with ZrO_2 reinforcement [4].

Sigworth and Kuhn [5] showed that Ti contributed to the grain refining mechanism by rising Al solidification temperature from 660.1 to 665 ^{o}C, at which $TiAl_3$ particles formed and initiated the cooling of Al melt to primary α-Al phase. $TiAl_3$ particles induced a heterogeneous nucleation of α-Al, hence a greater number of present $TiAl_3$ would refine the overall grain size. A research by Gao, et. al. [6] displayed an agreement to the statement, in which the addition of 0.2 wt. % Ti to Al-6Zn-2Mg-2Cu-0.2Zr wt. % alloy resulted in smaller α-Al grains in comparison to alloy samples without Ti addition. This is, however, limited to a certain time range during the cooling process before a *fading* event – submerging $TiAl_3$ intermetallic particles to the bottom of crucibles due to a prolonged holding time – occurs. On the occasion where intermetallic nuclei were unable to form, Ti would serve as a growth restricting agent [7]. The grain refining effect, by all mechanisms, will result in higher strength of the Al-alloy in accordance to Hall-Petch equation.

Further strengthening of Al 7xxx alloy is generally done through age hardening/T6 heat treatment method which consists of solution treatment, quenching, and ageing steps, producing precipitates of new phases that render dislocation movement. Possible identities of formed phases include GP Zone [8], η ($MgZn_2$), η' [9], β", $MgSi_2$ [10], cubic T' ($Mg_{32}(Al,Zn)_{49}$), and equilibrium T [11]. Reportedly, the addition of Ti was able to accelerate the precipitation forming in experimental ageing of Al-6Zn-2Mg-2.5Cu-0.2Zr-0.2Ti wt. % at 120 ^{o}C [6] and prevent grain boundary segregation from occurring during air cooling [9].

The above literature survey shows contributions of Ti alloying element to both as-cast and after age hardening properties of Al 7xxx alloy. Thus, the present work attempts to analyze the effects of Ti addition at varying

contents to the microstructure and mechanical properties of as-cast and age-hardened AlZnMg alloy.

2 Experimental methods

Al-10Zn-6Mg wt. % base alloys were produced using commercial pure Al (99.79 wt. %), Zn (99.99 wt. %), and Mg (99.90 wt. %) ingots with additions of Al-5Ti-B masteralloy rods at varying amounts to obtain final Ti content of 0.02, 0.05, and 0.25 wt. %. Starting materials were melted in a crucible furnace at 850 °C, degassed using argon gas for 1 min, and stirred immediately for 2 min. The melts were poured into a 170 x 170 x 15 mm^3 preheated metal mould followed with squeeze casting at 76 MPa for 10 min. Homogenisation was done at 400 °C for 4 h to uniform the microstructure of as-cast samples. Chemical composition of the Al-alloys determined by OES analysis using ARL 3460 OE Spectrometer is presented in Table 1. The alloys were then heat treated by T6 procedure consisting of solution treatment at 440 °C for 1 h followed with water quenching and ageing at 130 °C for 2-200 h. Samples for mechanical testing, microstructure, and phase characterizations were machined to prescribed test specifications.

Table 1. Chemical composition of as-homogenized Al-10Zn-6Mg-xTi wt. % alloys.

Sample	Zn	Mg	Ti	Fe	Al
A	10.318	6.741	0.004	0.172	*bal.*
B	9.701	6.734	0.018-0.0204	0.235	*bal.*
C	11.116	7.127	0.048-0.067	0.268	*bal.*
D	9.227	6.835	0.249-0.299	0.226	*bal.*

Mechanical testing was done through ASTM E 18 Rockwell B hardness testing and Charpy impact testing method. Zeiss-Primotech optical microscope and Zeiss SEM-EDS instrument were used for microstructural investigation on specimens prepared with standard metallographic preparation using 0.5 % HF etchant. Calculation of SDAS values were done on microstructure image of as-cast sample at 50 x magnification using ImagePro Analysis. Simultaneous Thermal Analysis (STA) was conducted to observe phase transformations, heat fluctuations, and alloys crystallinity as a function of time on temperatures on as-homogenized samples using STA 6000 Parkin Elmer at 30-750 °C with 10 °C/min scanning rate in accordance to ASTM E 168 standard.

3 Results and discussion

3.1 As-cast microstructures and hardness

Figure 1 presents the microstructures of Al-10Zn-6Mg alloys with various addition of Ti. Dendrites size decreased along with increasing content of Ti up to 0.25 wt. %. Microstructure of all samples, however, showed porosities occurring due to the existence of dissolved gas in the melting process. Eutectic phase β (Al_8Mg_5) was observed clearly inside the interdendritic phase. This is in agreement with the solidification sequence by Raghafan [12] which figured that Al-10Zn-6Mg alloy would form L + T at 480 °C and β at 448 °C, subsequently.

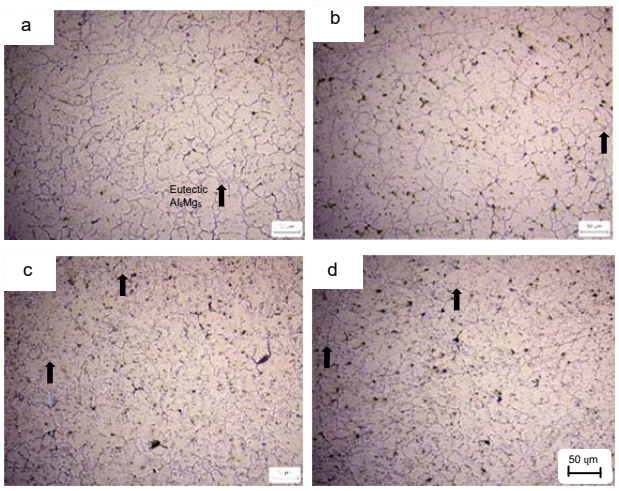

Fig. 1. Microstructure of as-cast Al-10Zn-6Mg alloy with : (a) 0, (b) 0.02, (c) 0.05, and (d) 0.25 wt. % Ti.

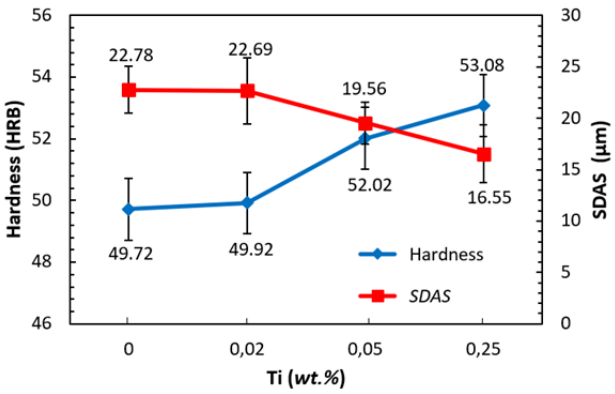

Fig. 2. The effect of Ti addition on hardness values and SDAS on Al-10Zn-6Mg-xTi alloys.

Ti addition affected the hardness and dendrites size of the alloy, as seen in Figure 2. As the addition of Ti increased, the SDAS values decreased while hardness of the alloy improved. Obtained SDAS values were 22.78, 22.69, 19.56, and 16.55 µm for the addition of 0, 0.02, 0.05, and 0.25 wt. % Ti, respectively. The hardness value increased gradually from 49.72 HRB to 49.92, 52.02, and 53.08 HRB, respectively for each Ti addition. Both results are related to each other. The addition of grain refiner promoted grain boundaries strengthening, thus improving the mechanical properties [3,4]. Grain refining action of Ti was achieved by the forming and distribution of $TiAl_3$ intermetallic phase in the melt, which became the nucleating place for α-Al. Another mechanism to note was the increasing of *Growth Restriction Factor* (GRF) due to the presence of solute Ti. The GRF value of the alloy escalated from 21 to 25.91, 33.28, and 82.4 at the addition of 0.02, 0.05, and 0.25 wt. % Ti respectively. Therefore, it can be inferred that grain refinement mechanisms of Ti in this alloy were α-Al nucleation and GRF escalation.

3.2 Effect of Ti on age hardening mechanism

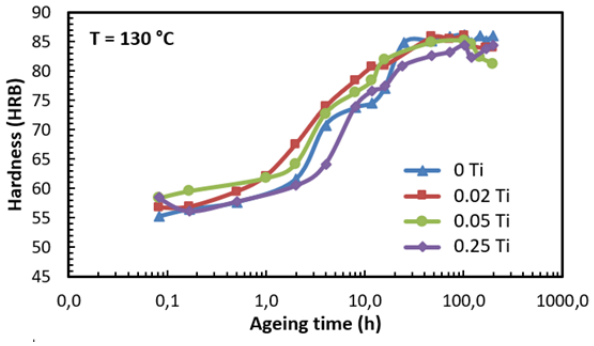

Fig. 3. Age hardening response of Al-10Zn-6Mg-xTi alloys at 130 °C for 200 h.

Age hardening response was observed in underaged, peakaged, and overaged conditions, of which hardness values can be seen in Figure 3. In the first 5 min, the alloys possessed underaged condition with hardness values of 55.3, 56.8, 58.3, and 58.4 HRB at addition of 0, 0.02, 0.05, and 0.25 wt. % Ti, respectively. Ti-doped alloys showed higher hardness values than those without. This is similar to a research by Gao, et. al. [6] which found that the presence of Ti accelerated initial ageing stage during artificial ageing at 120 °C, furthermore improved the hardness value. Peak ageing was observed at 102 h when hardness values of all samples significantly increased. However, sample without Ti addition showed higher hardness than Ti-added alloys. Alloys with 0, 0.02, 0.05, and 0.25 wt. % Ti had hardness values of 86.1, 85.9, 85.1, and 84.4 HRB, respectively. Moreover, the hardness values seemed to decrease as the Ti content was increasing. Therefore, it can be concluded that Ti did not induce either second phase or intermetallic phase formation at peakaged condition.

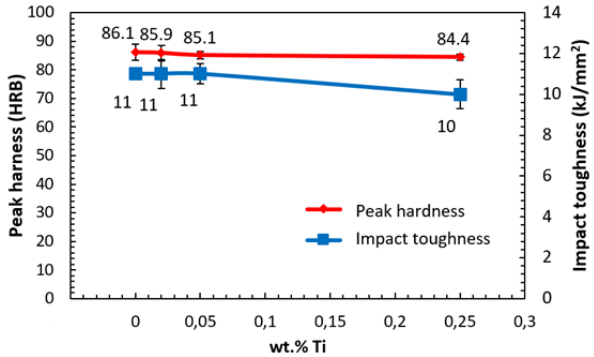

Fig. 4. Peak hardness and impact toughness values of Al-10Zn-6Mg-xTi at 130 °C.

Figure 4 illustrates the effect of 0, 0.02, 0.05, and 0.25 wt. % Ti addition on impact toughness and peak hardness of Al-10Zn-6Mg. It can be inferred that peak hardness and impact toughness were seemingly equal on all Ti variations; hence the addition of Ti contributed no significant effect on both aspects at peakaged condition. High level of hardness values at peakaged condition were a result of the formation of semi-coherent η' $MgZn_2$ precipitates in α-Al matrix. The precipitates distributed uniformly in the alloy during ageing furthermore inhibited dislocation movement due to deformation forces applied and improved the hardness value. Meanwhile, the addition of Ti, which contributed on reducing SDAS values, performed no effect on peak hardness. Instead, the formation of precipitates itself which took a big role on improving the mechanical properties. The images of fracture surface for each alloy with various Ti addition are shown in Figure 5. Fracture surface of alloys in as-aged condition were generally identified as brittle fracture. The images also show different grain fineness, where alloys with higher Ti content had finer grains.

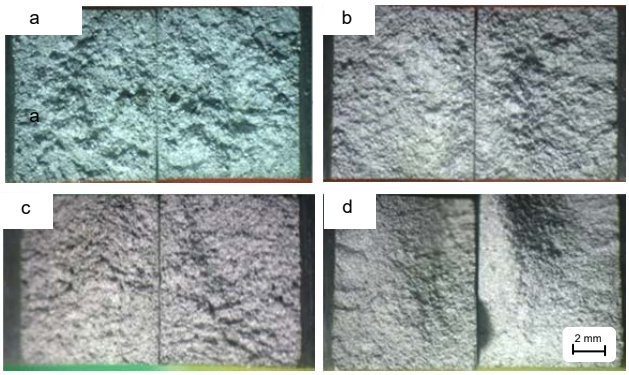

Fig. 5. Fracture surface of Al-10Zn-6Mg with addition of (a) 0, (b) 0.02, (c) 0.05, and (d) 0.25 wt. % Ti.

Microstructures of Al-10Zn-6Mg-xTi are shown in Figure 6. Interdendritic phase in white contrast and porosities in black contrast were observed in the structures. The number of interdendritic phase increased with more Ti addition. Porosities were formed due to the dissolution of hydrogen gas during casting process.

3.3 Phase transformation analysis with SEM/EDS

Figure 7 and Table 2 present the SEM images and EDX data of Al-10Zn-6Mg-xTi at peakaged condition. α-Al matrix, T ($Mg_{32}(Al,Zn)_{49}$), and β (Al_8Mg_5) were detected in Figure 7 (a-d). T phase was observed in cubic shape due to a low ratio of Zn:Mg. Interestingly, point 12 shows spider web-shaped cubic β phase inside the interdendritic structure. T and β phases were formed during the initial process of solidification. The low ratio of Zn:Mg caused η ($MgZn_2$) phase to be undetected in all alloy compositions. $TiAl_3$ was supposed to form in nanoparticle size that the morphology could not be observed. C and O_2 content was found in the alloy due to residual Al-SiC polishing cloth and paste (Al_2O_3).

3.4 Phase transformation analysis with STA

Phase transformation of the alloys can be seen through the endothermic and exothermic peak in Figure 8 (a-d). Reaction occurring in Al-10Zn-6Mg-xTi was SSSS → GP zone → η' → η [13]. Table 3 shows the formation (exothermic) and diffusion (endothermic) temperatures

of the alloys due to the heating process. Khrisna, et. al. [13] observed that the GP zone, η', and η developed at 20-120 °C, 120-150 °C, and 150-300 °C, respectively, while diffusion of each phases took place at 50-150 °C, 200-250 °C, and 300-350 °C, respectively, which are appropriate with findings in this work.

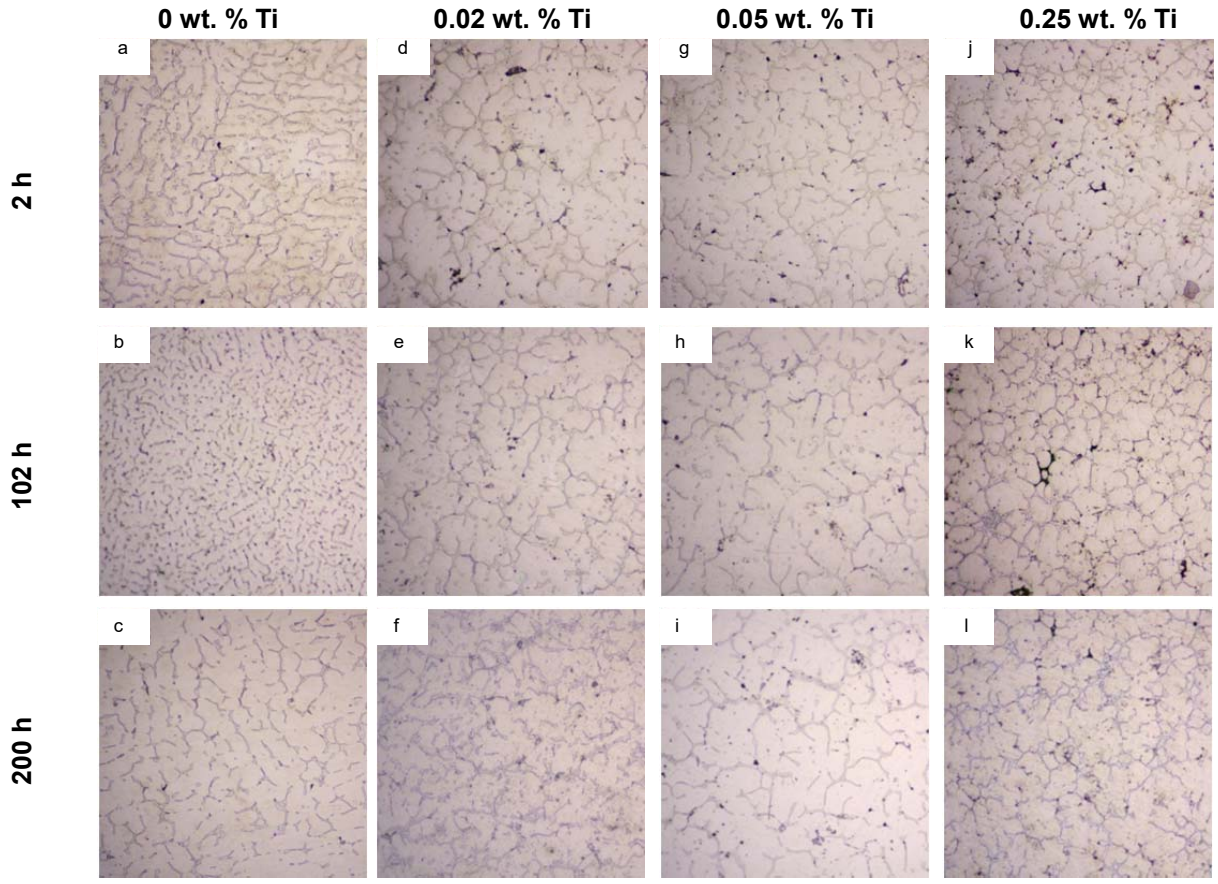

Fig. 6. Microstructure of Al-10Zn-6Mg alloy with: (a-c) 0, (d-f) 0.02, (g-i) 0.05, and (j-l) 0.25 wt. % Ti at underaged (2 h), peakaged (102 h), and overaged (200 h) condition with ageing temperature of 130 °C.

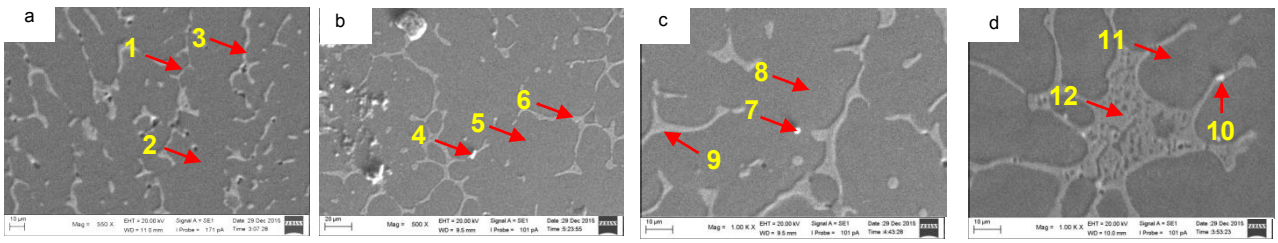

Fig. 7. SEM images of Al-10Zn-6Mg with addition of (a) 0, (b) 0.02, (c) 0.05, and (d) 0.25 wt. % Ti in peakaged condition.

Table 2. EDX characterization on Al-10Zn-6Mg-xTi

Mark	Element content (at. %)						Possible phase
	Al	Zn	Mg	Ti	C	O	
1	Bal	12.65	15.9	-	18.8	3.63	$Mg_{12}(Al,Zn)_{49}$
2	Bal	1.72	5.13	-	15.9	2.67	α-Al
3	Bal	1.84	5.22	-	14.9	2.87	Al_8Mg_5
4	Bal	0.68	2.23	1.83	45.8	36.1	$Mg_{12}(Al,Zn)_{49}$
5	Bal	-	1.52	0.05	46.3	37.9	α-Al
6	Bal	-	1.15	-	49.4	36.3	Al_8Mg_5
7	Bal	0.10	4.41	-	39.4	20.6	$Mg_{12}(Al,Zn)_{49}$
8	Bal	-	2.69	-	47.6	24.4	α-Al
9	Bal	-	4.17	-	29.9	9.89	Al_8Mg_5
10	Bal	13.09	20.9	-	24.1	6.80	$Mg_{12}(Al,Zn)_{49}$
11	Bal	-	4.24	-	29.5	13.3	α-Al
12	Bal	-	8.96	0.06	31.9	47.7	Al_8Mg_5

Table 3. Phase formation and diffusion temperature of Al-10Zn-6Mg-xTi.

wt. % Ti	Temperature °C		
	GP zone	η'	η
Formation			
0	40	120	200
0.02	40	150	190
0.05	40	120	210
0.25	40	180	360
Diffusion			
0	70	180	230
0.02	100	160-180	220
0.05	100	140	240
0.25	140	300	380

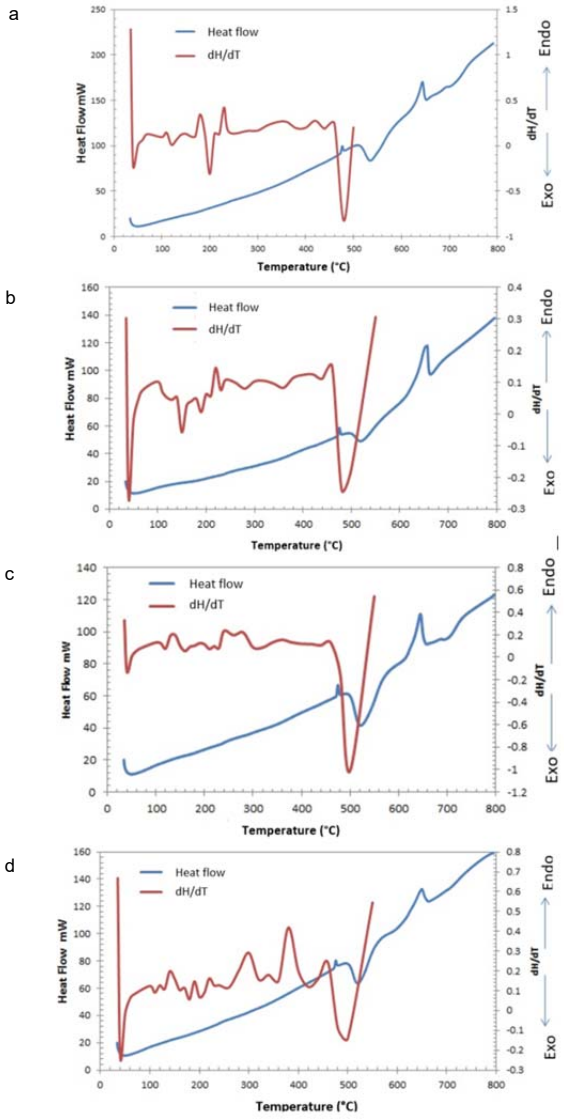

Fig. 8. Heat flow curves and their derivatives of Al-10Zn-6Mg with addition of (a) 0, (b) 0.02, (c) 0.05, and (d) 0.25 wt. % Ti.

Results of STA analysis in this work showed that formation of GP zone, *η'*, and *η* occurred at 40 °C, 120-180 °C, and 190-360 °C, respectively. The diffusion of GP zone took place at 70-140 °C, *η'* at 140-300 °C, and *η* at 220-380 °C. In addition, the heat flow curves showed two endothermic peaks. The first one was indicated as β phase diffusion, which occurred at 476.67, 475.43, 475.25, and 475.85 °C for alloy with 0, 0.02, 0.05, and 0.25 wt. % Ti, respectively. β phase was formed at 447 °C. Additionally, the second endothermic peak presented the α-Al phase diffusion for each alloy with 0, 0.02, 0.05, and 0.25 wt. % Ti which were at 644.06, 656.53, 645.05, and 649.23 °C. It was lower than 660 °C due to alloying content which decreased the melting point of base metal. In summary, Ti addition gave no effect on the temperature of phase transformation.

4 Conclusions

This work investigated the microstructure, phase transformations, and mechanical properties of aged Cu-10Zn-6Mg alloys with addition of 0.02, 0.05, and 0.25 wt. % Ti. Results are summarized as follows:

1. Addition of 0.02, 0.05, and 0.25 wt. % Ti increased the hardness of as-cast Al-10Zn-6Mg wt. % alloys from 49.72 to 49.92, 52.02, and 53.08 HRB, simultaneous to the reduction of its SDAS value from 22.78 to 22.68, 19.56, and 16.55 μm and a rise in GRF from 21 to 25.91, 33.28, and 82.4, respectively.
2. Ti did not contribute to the peak hardness of Al-10Zn-6Mg wt. % alloys which were found to be 86.1 HRB and 85.9, 85.1, and 84.4 HRB at 0.02, 0.05, and 0.25 wt. % Ti additions, respectively, proportional to their impact numbers, ranging between 10-11 kJ/m^2.
3. Microstructural investigation on Al-10Zn-6Mg-xTi wt. % alloys showed the presence of primary α-Al matrix, spider web-shaped β (Al_8Mg_5), and bright interdendritic T ($Mg_{32}(Al,Zn)_{49}$) phases.
4. Phase transformation during age hardening of Al-10Zn-6Mg-xTi wt. % alloys was identified as an exothermic formation of *η'* following the order of GP Zone → *η* → *η'* ($MgZn_2$) and its endothermic diffusion. The formation of β (Al_8Mg_5) was observed at 447 °C while its diffusion occurred at approx. 475 °C.

Acknowledgements

This work was supported by Directorate of Research and Community Services, Universitas Indonesia through Hibah PITTA (*Publikasi Internasional Terindeks untuk Tugas Akhir Mahasiswa*) UI 2018.

References

1. M. Syahid, B.T. Sofyan, J. Adv. Mat. Res. **789**, 324-329 (2013)
2. F.H. Kurniawan, *Pengaruh Penambahan 0.067, 0.081, dan 0.115 wt. % Ti thd Karakteristik Paduan AC4B Hasil LPDC* (Undergrad. Thesis, Universitas Indonesia, 2008)
3. B.T. Sofyan, D.J. Kharistal, L. Trijati, K. Purba, R. Susanto, Mat. Des. **31**, S-36-S43 (2010)
4. P.I. Lestari, *Studi Pengaruh Penambahan TiB terhadap Karakteristik Komposit Al-10Zn-6Mg-3Si Berpenguat ZrO_2 Hasil Squeeze Casting* (Undergrad. Thesis, Universitas Indonesia, 2009)
5. G.K. Sigworthh, T.A. Kuhn, *Grain Refinement of Aluminium Casting Alloys* (AFS, 2007)
6. T. Gao, Y. Zhang, X. Liu, Mat. Sci.&Eng. A **598**, 293-298 (2014)
7. B.T. Sofyan, L. Basuki, Proc. 11th Int. Conf. Quality in Research, 832-839 (2009)
8. B.T. Sofyan, *Pengantar Material Teknik* (Penerbit Salemba, 2009)
9. C.A. Grove, G. Judd, Met. Trans. **4**, 1025 (1973)

10. M. Murayama, K. Hono, Acta Mat. **47**, 1537-1548 (1999)
11. S.K. Maloney, K. Hono, I.J. Polmear, S.P. Ringer, Scripta Mat. **41**, 1031-1038 (1999)
12. V. Raghafan, J-Alloy Phase Diagrams. **28**, 203-208 (2007)
13. K.G. Khrisna, K. Sivaprasad, K. Venkateswarlu, K.C.H. Kumar, J. Mat. Sci. Eng. **535**, 129-135 (2012)